INDEX COPERNICUS INTERNATIONAL



Bio-Algorithms and Med-Systems

WWW.BAMSJOURNAL.COM ISSN: 1896-530X

SHORT COMMUNICATION

Received: 15.08.2024
Accepted: 22.11.2024
Published: 23.12.2024

CITE THIS ARTICLE AS:
Cesar JP, Abouzahr F, Crespo P, Gajda M, Kuo A, Mawlawi O, Morozov A, Ojha A, Poenisch F, Proga M, Sahoo N, Seco J, Takaoka T, Tavienier S, Titt U, Wang X, Zhu X, Lang K, "First PET Studies of a FLASH Proton Beam: Summary and Future Prospects" Bio-Algorithms and Med-Systems vol. 20, special issue, pp. 49-54, 2024, DOI: 10.5604/01.3001.0054.9140

AUTHORS' CONTRIBUTION:
A. Conceptualization
B. Data Curation
C. Formal Analysis
D. Funding Acquisition
E. Investigation
F. Methodology
G. Project Administration
H. Resources
I. Software
J. Supervision
K. Validation
L. Visualization
M. Writing – Original Draft
N. Writing – Review & Editing

CORRESPONDING AUTHOR:
John P. Cesar; University of Texas at Austin; Austin, TX 78712, United States; E-mail: john.cesar@austin.utexas.edu

COPYRIGHT:
Some rights reserved: Jagiellonian University Medical College. Published by Index Copernicus Sp. z o. o.

OPEN ACCESS:
The content of the journal „Bio-Algorithms and Med-Systems" is circulated on the basis of the Open Access which means free and limitless access to scientific data.

CREATIVE COMMONS CC BY:
Attribution. It is free to copy, distribute, present and perform the copyrighted work and derivative works developed from it, provided that the name of the original author is cited.

First PET Studies of a FLASH Proton Beam: Summary and Future Prospects

John P. Cesar[1BCEFJMN], Firas Abouzahr[1BCEL], Paulo Crespo[2,3ADE], Michael Gajda[1BCEFL], Alex Kuo[1BCEFL], Osama Mawlawi[4DHJ], Andrey Morozov[2ABCEIK], Aryan Ojha[1BCEFL], Falk Poenisch[4HJ], Marek Proga[1BEFL], Narayan Sahoo[4DGHJ], Joao Seco[5,6AE], Takeshi Takaoka[7HJ], Stefaan Tavienier[8DH], Uwe Titt[4HJ], Xiaochun Wang[4HJ], Xiaorong Zhu[4H], Karol Lang[1ABDEFGJ]

[1]University of Texas at Austin, Austin, United States
[2]Laboratório de Instrumentação e Física Experimental de Partículas, Coimbra, Portugal
[3]Departamento de Física, Universidade de Coimbra, Coimbra, Portugal
[4]MD Anderson Cancer Center, University of Texas, Houston, United States
[5]German Cancer Research Center (DKFZ), Heidelberg, Germany
[6]University of Heidelberg, Heidelberg, Germany
[7]Hitachi America Ltd, Houston, United States
[8]PETsys Electronics, SA, Taguspark, Portugal

ABSTRACT

Objectives: Proton therapy, while highly effective and successful, still lacks a key feature: the ability to assess, in-vivo, the dose and end-point location of irradiations. Known as proton range verification, this capability can be realized by incorporating positron emission tomography (PET) systems in both conventional and emerging modalities, such as FLASH proton therapy. FLASH itself may revolutionize radiation oncology with its purported ability to better spare healthy tissues, but only if the underlying mechanisms can be understood. We summarize our work towards establishing in-beam PET modalities and elucidating the mystery of the FLASH effect.

Materials: We've developed a PET scanner designed for live, in-beam imaging during therapeutic proton irradiations that can use short-lived positron emitting species (PES) activated by the beam to validate the range and dose of proton depositions. This scanner is made up of PET modules consisting of arrays of LYSO (lutetium-yttrium oxyorthosilicate) scintillating crystals coupled one-to-one to silicon photomultiplier (SiPM) arrays. These modules are readout by electronics based on the TOFPET2 ASIC platform from PETsys Electronics.

Methods: Our collaboration with MD Anderson Cancer Center has given us opportunities to take real in-beam data using a non-clinical beamline capable of delivering FLASH proton irradiations into target phantoms made of polymethyl methacrylate (PMMA), high density polyethylene (HDPE), and water. Data collected both during and afterirradiations were used to perform novel analyses and to reconstruct images of PES activity due to the beam.

Results: Exploratory studies, using a subset of our PET scanner, have demonstrated successful data acquisition during and after FLASH beam spills including quantitative

imaging and dosimetry of activated phantoms. The full results, explored in this work, are highly promising and prove that in-beam PET can deliver on its goals. Upcoming experiments conducted using both FLASH and conventional beams will employ the full PET scanner and involve a rich experimental program with novel ideas for irradiation targets, beam characterization, and in-depth comparisons of the two irradiation modalities.

Conclusions: This work demonstrates the unprecedented proof-of-principle for the capabilities of an in-beam PET scanner for imaging and dosimetry of both conventional and FLASH proton beams. These results open a new PET modality with proton beams which is particularly attractive for FLASH therapy but can serve effectively all proton irradiations, leading to improved treatment monitoring and image-guided therapy.

KEYWORDS

PET, Proton Therapy, FLASH, Image-Guidance, Proton Range Verification

LIST OF ABBREVIATIONS

CTR – coincidence time resolution
FOV – field of view
HDPE – High-Density Polyethylene
LYSO – lutetium-yttrium oxyorthosilicate
MDACC – MD Anderson Cancer Center
PES – positron-emitting species
PET – positron emission tomography
PMMA – polymethyl metacrylate
SiPM – Silicon Photomultiplier
ToF – time of flight
TPPT – time-of-flight PET for proton therapy

OBJECTIVE

The concept of monitoring and assessing a therapeutic proton beam, while not new, has been lacking concerted effort to realize its potential to alleviate one of the most fundamentally important issues in all of radiation oncology: treatment induced toxicity in healthy tissue. In order for proton therapy to truly exploit its advantage over photon-based radiation treatments via the characteristic Bragg Peak in its depth-dose curve [1], a detailed characterization of each irradiation's stopping position within a patient is required. Known as proton range verification, this capability can be realized by surrounding a patient with dedicated, highly sensitive instruments that can detect the secondary particles arising from the interaction of the proton beam with the tissues of a patient.

Positron emission tomography (PET) scanners are one natural choice in this endeavor, since the proton beam itself will create, along its path through tissues, positron-emitting species (PES), which can be recorded and imaged with such a scanner [2–14]. These short-lived isotopes, such as ^{10}C, ^{11}C, ^{13}N, and ^{15}O, all have half-lives between approximately 20 s and 20 min, and thus must be measured immediately following a beam irradiation to acquire enough statistics and to avoid biological washout.

The idea of proton range verification becomes even more important in the context of FLASH proton therapy. FLASH radiation therapy in general, which involves delivering radiation at ultrahigh doses and dose rates (on the order of tens or hundreds of Gray deposited in fractions of a second), appears to be just as effective at eradicating tumor cells while, simultaneously, being better at sparing healthy tissue cells [15–26]. This paradoxical effect, observed and confirmed in small animal studies, is not yet understood by researchers and is a main obstacle to the trial and use of this modality in treating tumors in humans. By using an in-beam PET system in conjunction with a FLASH proton beam, we aim to demonstrate that even under conditions of very high doses and dose rates, PET image-guidance can be achieved and may open the door to its use in helping to understand the FLASH effect.

MATERIAL

The time-of-flight PET for proton therapy (TPPT) consortium has developed a PET scanner capable of operating in close spatial and temporal proximity to a proton beam so that it may use the short-lived radioactive isotopes activated by the beam to validate the range and dose of proton depositions during each irradiation [27, 28]. The TPPT scanner was designed to have high resolution and high sensitivity and uses fast electronics to implement time of flight (ToF) information during image reconstruction to achieve high fidelity even with limited statistics. Additionally, the TPPT scanner avoids interfering with the proton beam itself by employing partial ring geometry with gaps for the beam.

The TPPT scanner is made up of two halves in the shape of angular sections of a torus. When brought together they form a partial ring with an inner diameter of 325 mm, an axial length of 105 mm and with each half subtending an angle of 99 degrees. A photograph

of the scanner is shown on the left in Fig. 1., which depicts the two scanner halves around a model human head. Each detector crescent is made up of 48 modules (so-called TPPT modules, shown on the right in Fig. 1.) consisting of two 8 × 8 LYSO arrays (with crystal dimensions of 3 mm × 3 mm × 15 mm) coupled one-to-one to Hamamatsu Silicon Photomultiplier (SiPM) arrays. The readout electronics have been supplied by one of the consortium members, PETsys Electronics, and is based on their proprietary TOFPET2 ASIC, designed specifically for applications with high data rates, which require fast timing [29]. The full TPPT scanner is in the final stages of calibration and optimization in preparation for in-beam studies. Results of characterizing the scanner have yielded a coincidence time resolution (CTR), a performance metric for ToF-PET scanners, of approximately 230 ps (or approximately 180 ps when geometrically optimized for best lines of response). Time alignment and normalization calibrations are underway and further optimization may improve these values further.

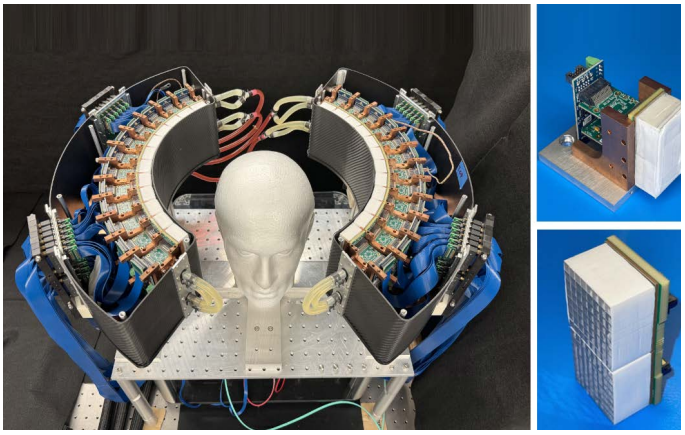

Fig. 1. Photographs of the full TPPT Scanner (left, shown with top cover panels removed) and the modules that comprise it (right).

METHODS

Our experiments were carried out at MD Anderson Cancer Center's (MDACC) Proton Therapy Center, where a non-clinical fixed ocular beamline, now used primarily for research, has been modified by the center's staff to allow delivery of FLASH irradiations [30, 31]. The beam is created from a Hitachi medical synchrotron producing a beam with energy of 75.8 MeV at the aperture used for these experiments. The intensity of the beam is flat to within 2–3% across a circular profile of the beam with a diameter 16 mm, and it falls off to approximately 80% at 20 mm in diameter. The FLASH extraction or "spill" lasts about 101.5 ms and delivers about 3.5×10^{10} protons for a dose of about 164 Gy s^{-1}. Since these experiments were performed in parallel with the assembly and commissioning of the full TPPT scanner, only two spare TPPT modules were available to create a "mini-PET" scanner which could surround small cylindrical phantoms placed along the beam axis, as shown in Fig. 2. A number of different materials were used for these phantoms in order to study the activation of different PES. A full summary of the various phantoms and runs taken can be found in the full publications regarding these experiments, and we focus on selected highlights here [32, 33].

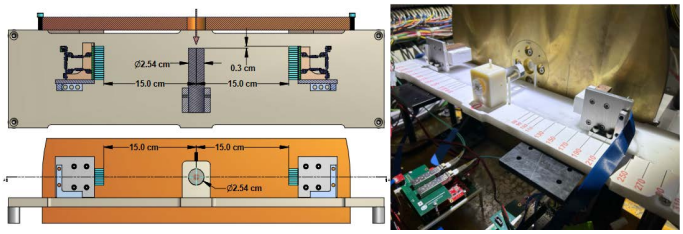

Fig. 2. Renderings (left) and photograph (right) of the setup used to acquire PET coincidence data from FLASH beam irradiations at MD Anderson Cancer Center. The PET system consists of two TPPT modules placed on either side of a target phantom being irradiated by the beam.

RESULTS

Our first exploratory in-beam studies of the FLASH proton beam at MDACC introduced us to the beamline and the space in which we could conduct our experiments. Although these first runs verified that our TPPT modules could withstand the high--radiation environment and successfully record and create an image of the PES activated in our phantoms by the FLASH beam, they also illustrated two issues in our setup: (1) nonoptimal alignment between our modules and the phantoms meant that very little PES activity was being captured in the field of view (FOV) of our setup, and (2) our electronics were not able to record any data during the FLASH beam spill due to saturation effects. These two issues are illustrated in Fig. 3. With this knowledge in hand, we designed a significantly better experimental setup for our second visit to MDACC (the setup shown previously in Fig. 2.) and also swapped some of our readout electronics for components which have higher bandwidth capabilities. The improved results obtained from these higher quality data are summarized below.

During this second experimental campaign, we collected PET data in coincidence mode from our two TPPT modules for up to 20 min after

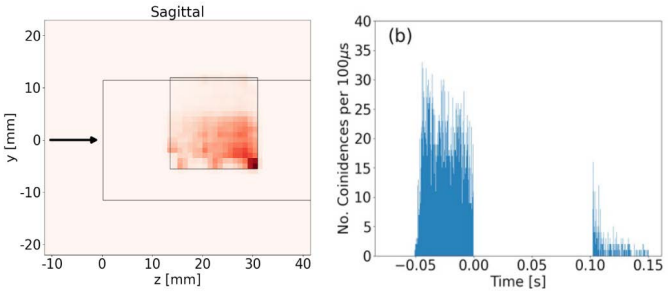

Fig. 3. Illustration of the two main issues discovered during our first studies with the FLASH proton beam at MDACC. The left plot shows a sagittal view (looking along the axis connecting the two TPPT modules) reconstruction of PES activity in a phantom. The smaller square outline is the FOV of the system, while the larger rectangular outline denotes the boundaries of the phantom. Thus, much of the activity in the phantom is outside the FOV of the detectors. The right plot shows PET coincidence events versus time and a gap during the 101.5-ms beam spill due to saturation of the readout electronics.

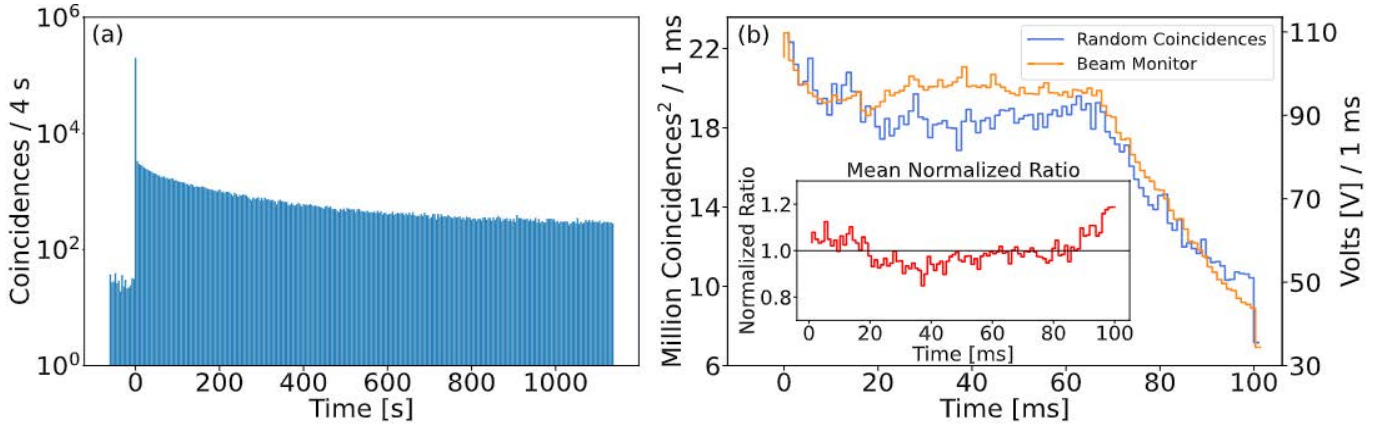

Fig. 4. On the left is an example of a full time series of PET coincidence events collected during a typical run. The sharp peak around the zero-seconds mark is due to the FLASH beam spill, while the decaying exponential trend that follows it is typical of PES activity. On the right is a plot comparing the beam monitor output with a proxy constructed from our in-spill PET coincidences, as described in the text.

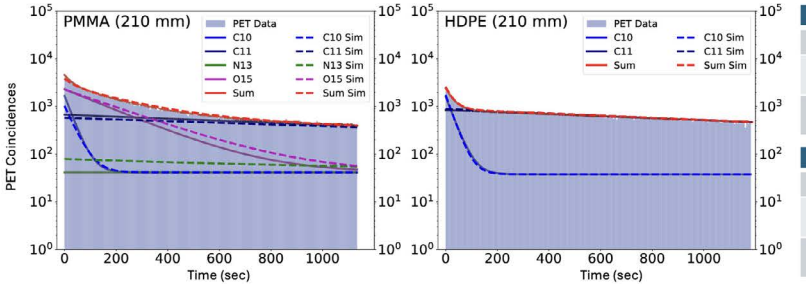

Phantom	PMMA ($C_5H_8O_2$)$_n$				
Isotope ($T_{1/2}$)	^{10}C (19.3 s)	^{11}C (1220.4 s)	^{15}O (122.4 s)	^{13}N (597.9 s)	χ^2/ndf
Fitted Rel. Abundance	0.36	0.14	0.50	< 0.01	1.29
Simulated Rel. Abundance	0.26	0.14	0.59	0.01	-

Phantom	HDPE (C_2H_4)$_n$				
Isotope ($T_{1/2}$)	^{10}C (19.3 s)	^{11}C (1220.4 s)	^{15}O (122.4 s)	^{13}N (597.9 s)	χ^2/ndf
Fitted Rel. Abundance	0.66	0.34	-	-	1.33
Simulated Rel. Abundance	0.67	0.33	-	-	-

Fig. 5. Collected PET coincidence time series following FLASH irradiations of PMMA (left) and HDPE (middle) phantoms. The colored solid and dashed lines show the results of fitting or simulating, respectively, contributions from different positron emitting isotopes activated by the beam. The tables on the right summarize these fit and simulation results, which are in good agreement with one another and with the data.

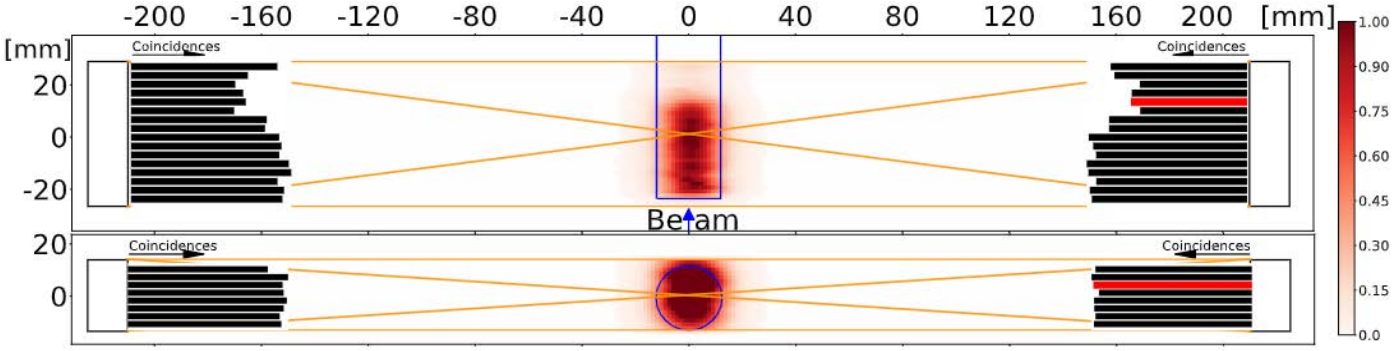

Fig. 6. Reconstructed PET images of PES activity in an irradiated phantom from coronal (top) and axial (bottom) views. The cylindrical phantom is outlined in blue (rectangular from the coronal view and circular from the axial view), while the orange lines denote the FOV boundaries. The black rectangles on either side of each image denote our TPPT modules, and the black bars represent the sum of coincidence counts in columns or rows of pixels (where a red bar denotes that a given column or row was found to have a potentially dead or noisy pixel included).

each FLASH beam spill into a phantom. A sample time series, which includes both in-spill and post-spill coincidences, is shown on the left in Fig. 4. In this new data the in-spill portion no longer has temporal gaps, where data is missing due to saturation issues. We were able to use these in-spill events, which are due to random coincidences between prompt gammas, to construct a proxy for the beam intensity during the spill. By taking the squared rate of these random single-hit coincidences in 500 ps time windows, the resultant time series agrees very well with data from an upstream beam monitor (as shown in the right plot of Fig. 4.). The post-spill data show the expected exponential decay trend due to the short half-lives of the activated positron emitters. By isolating these post-spill events we were able to fit these histograms to obtain estimates of the relative abundance of different positron emitting isotopes activated within our phantoms. An example of this analysis is shown in Fig. 5. for two of our phantoms, one made from PMMA plastic and the other from HDPE plastic, and the results agree very well with simulations based on Geant4 [34]. The primary goal of proton range verification, as the name implies, is to reveal the end point of the beam. To that end our analysis also included imaging and dosimetry of the activated positron emitters created by the beam (which can be correlated back to the proton dose distribution). We used the

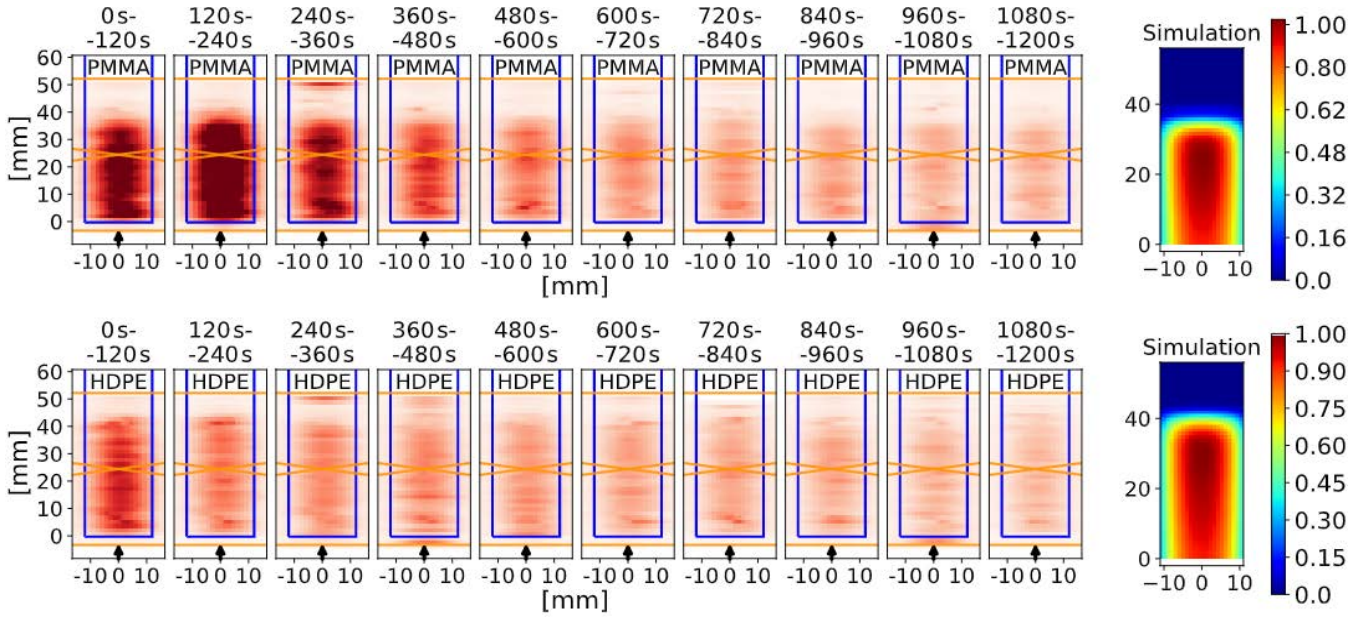

Fig. 7. These are "snapshots" of coronal PET images reconstructed from 120-s time intervals (as denoted above each frame), in PMMA (top) and HDPE (bottom) phantoms. As in the previous image, blue lines denote the phantom boundaries, while orange lines denote the FOV boundaries. The Geant4 simulated PES activity produced by the beam is shown to the right for each phantom.

CASToR program to reconstruct images of the PES activity within our phantoms [35]. Even with improvements to our experimental setup for our second campaign, the two TPPT modules employed could only afford us a very limited FOV for collecting PET events. Nonetheless, the reconstructed images, shown in Fig. 6., clearly show the range-out of the PES activity due to the finite penetration depth of the beam. In order to relate the PES activity distribution to the proton dose distribution, we have also used our comprehensive simulations to model the relation between these two distributions and compare it with our data, as shown in Fig. 7. We also note that Fig. 7., which shows reconstructed "snapshot" images using temporal slices of data 120 s long, demonstrates that even short PET acquisition times, on the order of a few minutes, should be sufficient to obtain valuable estimates of the proton beam range.

CONCLUSIONS

The work summarized here and presented as a contributing talk at the Fifth Jagiellonian Symposium on Advances in Particle Physics and Medicine demonstrates the feasibility, practicality and value of in-beam PET systems for assessing therapeutic proton beams. Even with the very limited exploratory setup that was employed we were able to successfully detect and create an image of the activated positron emitting species created by the beam in order to observe its penetration depth within our phantoms. Forthcoming studies with our full TPPT scanner will only yield a richer data set, which will allow us to properly quantify the proton beam's range and extract performance metrics for measuring key parameters of each irradiation.

In addition to exploiting the completed TPPT scanner in future studies, we are also designing a rich experimental program that will leverage the power of our technology to study novel phantoms and employ unique beam characterization ideas. Our studies will also involve irradiation using both conventional and FLASH proton beams so that we may better understand how to employ in-beam PET in both modalities and, we hope, how to help elucidate the mysteries of the FLASH effect.

Our results also demonstrate some of the other unique advantages of using PET as a tool for in-beam image-guidance, such as the ability to assess the composition of activated positron emitters in a target. To this end we are actively working with colleagues in the fields of biology and radio-biology to better understand how PET can be applied to potentially extract relevant information on how a tumor is responding to therapeutic irradiations as treatment progresses. This would further expand the nascent field of "image-guidance" in proton therapy to potentially also include "biological-guidance."

ACKNOWLEDGMENTS

We acknowledge support of this work by the University of Texas at Austin and the UT-Portugal program. We thank all members of the TPPT Consortium supported by the UT-Portugal Program at the University of Texas at Austin. The consortium involves researchers from the MD Anderson Cancer Center, PETSys Electronics and C^{2}TN in Lisbon, Portugal, LIP and ICNAS in Coimbra, Portugal and the group at University of Texas at Austin.

CONFLICT OF INTEREST

Authors have declared no potential conflicts of interest.

REFERENCES

1. Wilson RR. Radiological use of fast protons. Radiology. 1946;47(5):487–91. doi: https://doi.org/10.1148/47.5.487.
2. Parodi K, Enghardt W, Haberer T. In-beam PET measurements of β+ radioactivity induced by proton beams. Phys Med Biol. 2002;47(1):21–36.
3. Enghardt W, Crespo P, Fiedler F, Hinz R, Parodi K, Pawelke J, et al. Charged hadron tumour therapy monitoring by means of PET. Nucl Instrum Methods Phys Res. 2004;525(1–2):284–8.
4. Crespo P, Shakirin G, Fiedler F, Enghardt W, Wagner A. Direct time-of--flight for quantitative, real-time in-beam PET: a concept and feasibility study. Phys Med Biol. 2007;52(23):6795–811.
5. Zhu X, El Fakhri G. Proton therapy verification with PET imaging. Theranostics. 2013;3(10):731–40. doi: https://doi.org/10.7150/thno.5162.17.
6. Min CH, Zhu X, Winey BA, Grogg K, Testa M, El Fakhri G, et al. Clinical application of in-room positron emission tomography for in vivo treatment monitoring in proton radiation therapy. Int J Radiat Oncol Biol Phys. 2013;86(1):183–9. doi: https://doi.org/10.1016/j.ijrobp.2012.12.010.
7. Seco J, Clasie B, Partridge M. Review on the characteristics of radiation detectors for dosimetry and imaging. Phys Med Biol. 2014;59(20):R303–47. doi: https://doi.org/10.1088/0031-915/59/20/R303.
8. Paganetti H, El Fakhri G. Monitoring proton therapy with PET. Br J Radiol. 2015; 88(1051):20150173. doi: https://doi.org/10.1259/bjr.20150173.
9. Seco J, Spadea MF. Imaging in particle therapy: State of the art and future perspective. Acta Oncologica. 2015;54(9):1254–8.
10. Grogg K, Zhu X, Shih H, Alpert N, El Fakhri G. Proton Range Verification with PET Imaging in Brain and Head and Neck Cancers. J Nucl Med. 2018;59(supplement 1):658.
11. Krishnamoorthy S, Teo BK, Zou W, McDonough J, Karp JS, Surti S. A Proof-of-Concept Study of an In-Situ Partial-Ring Time-of-Flight PET Scanner for Proton Beam Verification. IEEE Trans Radiat Plasma Med Sci. 2021;5(5):694–702.
12. Parodi K, Yamaya T, Moskal P. Experience and new prospects of PET imaging for ion beam therapy monitoring. Z Med Phys. 2023;33(1):22–34.
13. Mryka W, Das M, Beyene EY, Moskal P, Stępien E. Estimating influence of positron range in proton-therapy-beam monitoring with PET. Phys Med Biol. 2023;19(1):96–100.
14. Baran J, Borys D, Brzeziński K, Gajewski J, Silarski M, Chug N, et al. Feasibility of the J-PET to monitor the range of therapeutic proton beams. Phys Med. 2024;118:103301.
15. Favaudon V, Caplier L, Monceau V, Pouzoulet F, Sayarath M, Fouillade C, et al. Ultrahigh Dose-Rate Flash Irradiation Increases the Differential Response Between Normal and Tumor Tissue in Mice. Sci Trans Med. 2014;6(245):245–93. doi: https://doi.org/810.1126/scitranslmed.3008973.
16. Fouillade C, Favaudon V, Vozenin MC, Romeo PH, Bourhis J, Verrelle P, et al. Hopes of high dose-rate radiotherapy. Bull Cancer. 2017;104(4):380–4.
17. Montay-Gruel P, Petersson K, Jaccard M, Boivin G, Germond JF, Petit B, et al. Irradiation in a flash: unique sparing of memory in mice after whole brain irradiation with dose rates above 100Gy/s. Radiother Oncol. 2017;124(3):365–9. doi: https://doi.org/10.1016/j.radonc.2017.05.
18. Vozenin MC, De Fornel P, Petersson K, Favaudon V, Jaccard M, Germond JF, et al. The advantage of FLASH radiotherapy confirmed in mini-pig and cat-cancer patients. Clin Cancer Res. 2019;25(1):35–42.
19. Vozenin MC, Hendry JH, Limoli CL. Biological benefits of ultrahigh dose rate FLASH radiotherapy: sleeping beauty awoken. Clin Oncol (R Coll Radiol). 2019;31(7):407–15.
20. Bourhis J, Montay-Gruel P, Gonçalves Jorge P, Bailat C, Petit B, Ollivier J, et al. Clinical translation of FLASH radiotherapy: why and how? Radiother Oncol. 2019;139:11–7. https://doi.org/doi.org/10.1016/j.radonc.2019.04.
21. Montay-Gruel P, Acharya MM, Petersson K, Alikhani L, Yakkala C, Allen BD, et al. Long term neurocognitive benefits of FLASH radiotherapy driven by reduced reactive oxygen species. Proc Natl Acad Sci U S A. 2019;116(22):10943–51.
22. Hughes JR, Parsons JL. FLASH Radiotherapy: Current Knowledge and Future Insights Using Proton- Beam Therapy. Int J Mol Sci. 2020;21(18):6492. doi: https://doi.org/10.3390/ijms21186492.
23. Fouillade C, Curras-Alonso S, Giuranno L, Quelennec E, Heinrich S, Bonnet--Boissinot S, et al. FLASH irradiation spares lung progenitor cells and limits the incidence of radio-induced senescence. Clin Cancer Res. 2020;26(6):1497–506. doi: https://doi.org/10.1158/1078-0432.CCR-19-1440.
24. Schuler E, Acharya M, Montay-Gruel P, Loo Jr BW, Vozenin MC, Maxim PG. Ultra-high dose rate electron beams and the FLASH effect: From preclinical evidence to a new radiotherapy paradigm. Med Phys. 2022;49(3):2082–95. doi: https://doi.org/10.1002/mp.15442.
25. Lin B, Gao F, Yang Y, Wu D, Zhang Y, Feng G, et al. FLASH Radiotherapy: History and Future. Front Oncol. 2021;11:644400. doi: https://doi.org/10.3389/fonc.644400.
26. Vozenin MC, Bourhis J, Durante M. Towards clinical translation of FLASH radiotherapy. Nat Rev Clin Oncol. 2022;19:791–803. doi: https://doi.org/10.1038/s41571-022-00697-z.
27. Cesar JP, Kuo A, Morozov A, Ojha A, Jesus B, Leong C, et al. Time-of-Flight PET for Range Verification in Proton Therapy. A poster at the IEEE Nuclear Science Symposium, Medical Imaging Conference, and Room Temperature Semiconductor Detector Conference 2022 (IEEE NSS MIC RTSD 2022). 2022 Nov 5–12; Milano Convention Centre, Milan, Italy.
28. Klein K, Matava W, Layden C, Sadam A, Lang K, Proga M, et al. Time-of--Flight PET for Proton Therapy (TPPT). A poster at the 12th International Conference on Position Sensitive Detectors. 2021 Sep 12–17; University of Birmingham. A poster at the 9th Conference on PET/MR and SPECT/MR and Total-Body PET Workshop, 2022 May 28–June 1; Isola d'Elba, Italy.
29. PETsys Electronics S.A., Taguspark, Ed. Tecnologia I, 24 and 26, 2740-257, Portugal.
30. Titt U, Yang M, Wang X, Iga K, Fredette N, Schueler E, et al. Design and validation of a synchrotron proton beam line for FLASH radiotherapy preclinical research experiments. Med Phys. 2022;49(1):497–509. doi: https://doi.org/10.1002/mp.15370.
31. Yang M, Wang X, Guan F, Titt U, Iga K, Jiang D, et al. Adaptation and dosimetric commissioning of a synchrotron-based proton beamline for FLASH experiments. Phys Med Biol. 2022;67(16):10.1088/1361-6560/ac8269. doi: https://doi.org/10.1088/1361-6560/ac8269.
32. Abouzahr F, Cesar JP, Crespo P, Gajda M, Hu Z, Kaye W, et al. The first PET glimpse of a proton FLASH beam. Phys Med Biol. 2023;68(12). doi: https://doi.org/10.1088/1361-6560/acd29e.
33. Abouzahr F, Cesar JP, Crespo P, Gajda M, Hu Z, Klein K, et al. The first probe of a FLASH proton beam by PET. Phys Med Biol. 2023;68(23). doi: https://doi.org/10.1088/1361-6560/ad0901.
34. Agostinelli S, Allison J, Amako K, Apostolakis J, Araujo H, Arce P, et al. GEANT4 – a simulation toolkit. Nucl Instrum Meth. 2003;506(3):250–303. doi: https://doi.org/10.1016/S0168-9002(03)01368-8.
35. Merlin T, Stute S, Benoit D, Bert J, Carlier T, Comtat C, et al. CASToR: a generic data organization and processing code framework for multi--modal and multi-dimensional tomographic reconstruction. Phys Med Biol. 2018;63(18):185005.